



Research Article

## An experimental investigation of an inclined solar chimney integrated into residential buildings with different materials construction for natural ventilation in a hot-arid climate

Benali OUSSAMA<sup>1,\*</sup>, Dobbi ABDELMADJID<sup>2</sup>, Hassini NOUREDDINE<sup>3</sup>,  
Mohamed El-Amine SLIMANI<sup>4</sup>, Hadjadj ABDESSAMIA<sup>5</sup>

<sup>1</sup>Underground Oil, Gas and Aquifer Reservoirs Laboratory, Department of Renewable Energies, Kasdi Merbah University, Faculty of Hydrocarbons, Renewable Energies and Earth and Universe Sciences, Ouargla, 30000, Algeria

<sup>2</sup>Department of Geology, Kasdi Merbah University, Faculty of Hydrocarbons, Renewable Energies and Earth and Universe Sciences, Ouargla, 30000, Algeria

<sup>3</sup>Department of Physics, University Abdelhamid Ibn Badis of Mostaganem, Faculty of Exact Sciences and Computer Science, Mostaganem, 27000, Algeria

<sup>4</sup>Theoretical and Applied Fluid Mechanics Laboratory, Department of Energetic and Fluid Mechanics, University of Science and Technology Houari Boumediene (USTHB), Algiers, 16111, Algeria

<sup>5</sup>LEVRES Laboratory, University of El Oued, Faculty of Technology, El Oued, 39000, Algeria

### ARTICLE INFO

#### Article history

Received: 17 February 2024

Revised: 22 July 2024

Accepted: 23 July 2024

#### Keywords:

Building Materials; Performance;  
Solar Chimney; Thermal  
Comfort; Thermal Inertia;  
Ventilation

### ABSTRACT

Solar chimneys are used to ventilate residential buildings, helping reduce infections caused by the recent COVID-19 pandemic. An experimental investigation was conducted to evaluate the efficiency of rooftop solar chimneys by assessing the thermal performance of two small rooms constructed from the two most commonly used building materials in the region: local stone and hollow brick. The study examined the effects of building materials, chimney inclination (angles of 30°, 45°, and 60°), and air gaps (0.15 m and 0.25 m) on the chimney's performance under real climatic conditions at the University of Ouargla, Algeria, known for its dry and hot climate, from May 8 to 13, 2021. The results showed that installation factors significantly affect the performance of solar chimneys. The inclination angle had the most significant impact, potentially enhancing performance by up to 20%. Additionally, selecting suitable building materials, such as local stone, for specific geographical areas can improve performance by at least 15% during peak times. The air gap, as a configuration factor, contributes to a 14% improvement in performance. The analysis revealed that the highest indoor air velocity in the living area can be achieved using a solar chimney with specific dimensions of 1 m x 0.65 m, an air gap of 0.25 m, and an inclination angle of 45°. At average solar radiation levels of 550, 800, and 950 W/m<sup>2</sup>, the solar chimney can achieve air change rates of 5, 6.5, and 7.8 air changes per hour (ACH), respectively.

**Cite this article as:** Oussama B, Abdelmadjid D, Noureddine H, Slimani MEA, Abdessamia H. An experimental investigation of an inclined solar chimney integrated into residential buildings with different materials construction for natural ventilation in a hot-arid climate. J Ther Eng 2025;11(3):643–658.

#### \*Corresponding author.

\*E-mail address: benali.oussama26@gmail.com

This paper was recommended for publication in revised form by  
Editor-in-Chief Ahmet Selim Dalkılıç



## INTRODUCTION

The private and public building sectors are significant energy consumers, as they require energy to provide optimal comfort for the occupants of the buildings. The energy demands of the building sector are consistently rising to satisfy people's indoor comfort needs. Declining fossil fuel reserves due to increasing consumption and rising energy demand have forced Algerian policymakers to explore new sources of energy production. The building sector in southern Algerian regions is known for being energy-intensive. According to a report from the National Agency for the Promotion and Rationalization of the Use of Energy (APRUE), energy consumption in the construction and agriculture sector constitutes 46.7% of the total energy consumption, surpassing both the transport sector (30.6%) and the industry sector (22.7%) [1]. During the summer season in the Algerian Sahara, there is a significant increase in the demand for energy to power air conditioning systems. Due to the extremely hot climate experienced during this period, energy consumption in buildings is on the rise in developing countries like Algeria [2].

Using energy-efficient materials in construction has been extensively studied as a potential solution [3], reducing the energy consumption of space-conditioning systems, this can help minimize the negative impacts of severe outdoor weather conditions on building occupants and improve indoor thermal comfort [4]. When selecting building materials, it is necessary to choose materials that help reduce energy consumption, contribute to reducing CO<sub>2</sub> emissions, and achieve the required thermal comfort in buildings. Local building materials and traditional construction are two important energy-saving solutions; these solutions can immediately achieve zero energy balance and zero local carbon dioxide emission in Mediterranean climates [5, 6]. To reduce energy use for space cooling, heating, and air conditioning, studies have focused on evaluating and analyzing the thermal efficiency of the building envelope. Studies have confirmed that the design and structural properties of the envelope, and the thermal and physical properties of the materials used for construction affect the environmental and energy performance of the building, which interact and communicate with external climatic conditions [7, 8]. The study assessed the thermal response times for walls constructed from cut stone in a historical building and compared them to those made from modern brick and gas concrete. It established the necessary insulation thicknesses for these materials to meet U-values of 0.6, 0.4, and 0.2 W/m<sup>2</sup>. K. There were noticeable differences in internal temperature changes, with aerated concrete experiencing the highest fluctuation at 0.59°C and cut stone the lowest at 0.18°C. The results demonstrate that walls with higher thermal inertia are better at resisting changes in external temperatures, even though they have relatively high U-values. This implies that the substantial thickness of walls in historical buildings is designed to increase thermal

inertia, enhancing thermal comfort and reducing energy loss [9]. The results show that to minimize the energy consumption of the building envelope, the optimal combination of parameters is a window-to-wall ratio of 7%, the use of triple-glazed glass, shading with an overhang fin, and west orientation. Among these factors, the window-to-wall ratio is the most influential. By optimizing these parameters, architectural designers can significantly reduce the energy demand of buildings, providing more efficient solutions for energy-efficient construction [10]. The building envelope is an important factor as a passive source of energy. To achieve better thermal comfort in arid and hot areas, Bekkouche et al. [11] showed that the horizontal position of hollow bricks gives the best results. Among the solutions, natural ventilation of buildings is important to avoid thermal discomfort. Natural ventilation is an economical and inexpensive solution [12]. The researchers emphasized the importance of orientation in non-air-conditioned buildings and its impact on the building's internal thermal comfort standards. The study concluded that the impact of changing direction relates to floor and envelope building materials, insulation levels, and following bioclimatic design rules [13]. Researchers noted that when phase change materials (PCMs) are integrated into envelope systems based on orientations and seasons, it is possible to reduce annual energy consumption by more than 50% and reduce demand for cooling and heating [14]. The authors discuss strategies for enhancing living conditions inside a semi-buried building in a hot and arid climate. Temperature predictions for this setup were modeled using the ANSYS-Fluent software. The findings indicate that in the buried part of the room, at a height of 2 m, the temperature remains below 25 °C, while in the non-buried part between the heights of 2 and 3 m, it varies between 25 and 26 °C. This thermal behavior inside the room ensures effective cooling with minimal electrical energy usage [15].

In the past, researchers have pursued new methods to reduce energy usage in building design. One such method is bioclimatic design, which involves integrating energy-saving strategies into construction and utilizing renewable energy sources like solar power [16]. Traditional heating, cooling, and ventilation systems consume substantial energy in residential areas. To mitigate this, a passive design approach is preferred to reduce reliance on mechanical systems and overall energy demand during construction. Solar chimneys represent an innovative passive design solution that harnesses solar energy to create a natural updraft through chimney ducts. This approach enhances environmental quality and indoor air conditions within buildings, improving thermal comfort efficiency while significantly lowering carbon dioxide emissions [17]. Among the main recommendations to reduce energy consumption in buildings is the use of solar passive ventilation systems, such as improving solar energy gain by changing the orientation of the building, and solar chimneys can be installed on walls and roofs. The device consists of a transparent cover, a black

panel, and an air inlet and outlet connected to the roof. By exploiting solar thermal energy, it is possible to establish an acceptable temperature differential between the air within and outside the solar chimney channel and to use the buoyancy effect to induce a ventilation flow. Due to its use of renewable energy, low operating costs, and absence of carbon dioxide emissions compared to mechanical ventilation systems, the solar chimney is a bioclimatic design for sustainable development [18]. The studies on solar chimneys aimed to enhance natural ventilation by analyzing different design elements. The effects of absorber materials, position, and design configurations of solar chimneys were considered. Research indicates that many studies in the field exclusively utilized experimentation or an experimental approach in conjunction with numerical modelling [19]. According to the empirical findings about the design configuration of Afonso and Oliveira [20], the chimney width had a more significant impact on the ventilation rate than its height. Studies conducted by Mathur et al. [21] revealed that there is a direct relationship between the ventilation rate and the ratio between the absorber height and the gap between the glass and the absorber, and the researchers found that a stack height-to-air gap ratio of 2.83 for a chimney with a height of 1 m gives the highest ventilation rate.

While Hamdy and Fikry [22] found that the ideal inclination angle for the proposed model was  $60^\circ$  to provide optimal ventilation performance. The effect of heat flux and inclination angle on the thermal efficiency of a solar chimney integrated into the building was studied using phase change material (PCM) as an insulator. An experimental research was conducted to achieve this objective. The effect of three different inclination angles on the chimney's performance was studied at different heat fluxes. The study results indicate that the inclination angle affects the buoyancy effect and natural convection within the PCM. The values of the chimney performance and airflow were highest at  $45^\circ$  in studied cases, and the airflow increases with the increase in the heat flux value [23].

The researchers conducted an optimization study and concluded that the solar chimney with the following dimensions: 1.85 m height, 2.65 m width, an inclination angle of  $75^\circ$ , and an air gap of 0.28 m, achieves the highest values of indoor air velocity in a residential building. Sensitivity analyses indicate that the width of the solar chimney is the most influential factor, while the height of the solar chimney is not an influential factor compared to the rest. The proposed solar chimney can generate air velocities of up to 0.28, 0.47, and 0.52 m/s when exposed to average solar radiation values of 500, 700, and 850  $W/m^2$ , respectively [24]. The statistical analysis of the experimental study results indicates that the total number of tests conducted is relatively small. Therefore, more necessary tests and research must be carried out to enhance the performance of the rooftop solar chimney. It is recommended to combine the following features: a high cavity with potential for solar radiation, a cavity gap measuring 0.2–0.3 m, equal

inlet and outlet, a height-to-gap ratio of approximately 10, a tilt angle of  $45^\circ$ – $60^\circ$ , an adequate-sized room opening, double or triple glazing, a 5 cm thick insulation wall, and a solar absorber with high absorptivity and emissivity [25]. By identifying the elements that affect the performance of solar chimneys in buildings, the results showed that choosing the ideal inclination angle for the chimney significantly improves ventilation rates. Furthermore, by reducing the inclination angle from  $80^\circ$  to  $20^\circ$ , the maximum air mass flow rate increases from 0.06 to 0.14 kg/s. When compared with solar chimney ventilators with an inclination angle of  $80^\circ$ , the energy saving performance of those with an inclination angle of  $20^\circ$  is approximately 144% greater. The performance of the chimney from sunrise to noon is best at an inclination angle of  $40^\circ$  [26]. The study investigated the impact of various factors on the performance of the solar chimney, including the depth of the air gap, the size of the openings, the external air temperature, and solar radiation, to identify optimal operating conditions that meet thermal comfort standards. The findings indicated that the chimney effectively maintains indoor air conditioning throughout the day. Notably, even under conditions of low solar intensity ( $215 W/m^2$ ) and a cool ambient temperature ( $5^\circ C$ ), the chimney achieved an air change rate of 2.93 air changes per hour (ACH) [27]. An experimental and numerical study was conducted on the efficiency of a rooftop solar chimney in a room of 12  $m^3$  volumes. Solar radiation of  $750 W/m^2$  was applied to the facade of the chimney, the aspect ratio was 13.3 and the chimney's height was 2 m. The results showed that the ventilation rate is highest at an inclination angle of  $60^\circ$ . The ventilation rate at  $60^\circ$  was 30 ACH, about 20% higher than at  $45^\circ$  in a 12  $m^3$  room, and the maximum air velocity was 0.8 m/s at an air gap of 50 mm [28]. The jet impingement method is highly effective for enhancing convective heat transfer in solar chimneys. The study focuses on a new jet plate solar air heater, design enhanced with continuous longitudinal fins, which significantly improves convective heat transfer in applications like space heating, crop drying, and building heating. Performance evaluations based on heat transfer and pumping power (represented by the Nusselt number and friction factor) across Reynolds numbers from 2500 to 18,000 show that this new design of solar air heater jet impingement (SAHJI) increases heat transfer by 1.65 times and achieves superior hydraulic performance compared to a traditional smooth solar air heater (SSAH) [29]. Based on the authors' survey and previous studies, there have been few empirical investigations into rooftop inclined solar chimneys and the influence of external factors on their efficiency. This study specifically focuses on the impact of optimal construction materials on chimney performance, an aspect that has not been previously addressed and represents the original contribution of this research. Therefore, the authors conducted an examination of rooftop solar chimneys under real climatic conditions, particularly in a region known for its hot and dry climate. These conditions typically diminish the device's

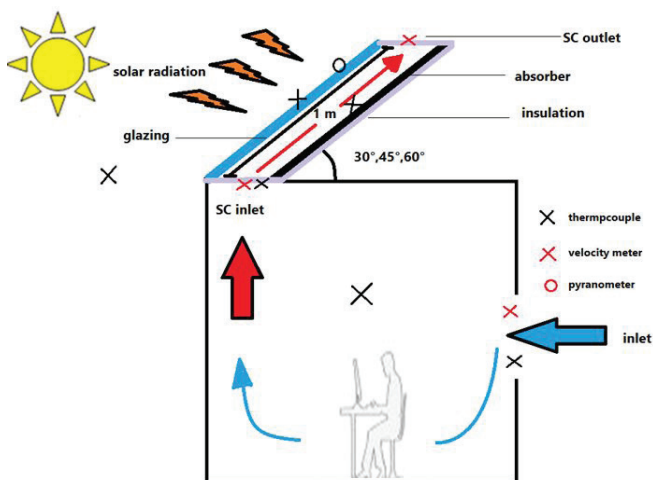
performance by failing to create the necessary thermal difference between the inlet and outlet temperatures of the chimney required to stimulate air movement and achieve adequate ventilation. This study was conducted to explore a solution that enhances the temperature differential between the outside and inside the room and increases the chimney performance level. For this purpose, the research evaluated the rooftop solar chimney connected to two small rooms, each built from different materials: local stone and hollow bricks, at various inclination angles and with different air gaps, all under real climatic conditions. This study aims to investigate the impact of various factors on the air movement and ventilation performance of chimneys. Specifically, the effects of building materials, inclination angle, and air gap on chimney performance will be examined by monitoring air movement, evaluating the comfort zone, and determining the air changes per hour (ACH) the chimney can achieve.

## EXPERIMENTAL SETUP

The study aims to enhance a passive ventilation system that improves indoor air quality and reduces energy consumption. This system operates using renewable energy and includes an inclined solar chimney, integrated into the building as shown in Figure 1. A solar chimney is a device used for ventilation that extracts air from an enclosed space by exploiting the density difference between hot and cold air. This system facilitates ventilation using clean, free renewable energy sources. Initially, the researchers investigated the thermal performance of two small rooms made of two different building materials widely used in the Algerian Sahara, namely hollow brick and local stone, as shown in Figure 2. The objective was to identify a building material that would help reduce energy consumption and enhance comfort. In the second stage, the performance of solar-assisted ventilation technology was analyzed in these two



(a) Images of the model



(b) Model layout

**Figure 1.** Experimental setup.



**Figure 2.** Construction process of the cubicles (a) hollow brick (b) local stone.

rooms in Ouargla city, Algeria (31°56'60"N, 5°19'0.001"E), under real weather conditions. The study examines and compares the performance of six ventilation scenarios. Measurements were conducted from 8:00 AM to 6:00 PM over six consecutive days, starting from May 8, 2021. The region is characterized by a hot and dry climate, with high temperatures in summer.

**Experimental Cavities**

One of the main objectives of this research is to identify a local building material that helps rationalize and reduce energy consumption by conducting a thermal performance analysis of two common materials widely used in the southern region of Algeria: local stone and hollow brick. Figure 2

provides an overview of the small rooms used in this study. Each room has dimensions of 1 m × 1 m × 1 m. The rooms feature a laminated wooden door (0.65 m by 0.3 m) on the east wall and a single-pane window (0.35 m by 0.35 m) on the north wall.

The construction components of the two rooms, along with the physical characteristics of each material, are detailed in Tables 1 and 2. The physical characteristics of the stone and brick were measured in a laboratory at the University of Ouargla.

**Solar Chimney**

To integrate the solar chimney onto the rooftop of a residential room, an opening measuring 0.25 m by 0.60 m

**Table 1.** Components of the brick cubicle room [45]

Wall	Composition	e (cm)	ρ (kg/m <sup>3</sup> )	Ci (kJ/ kg. K)	k (W/m.k)
Vertical walls	Mortar	1.5	1700	1	1.15
	hollow brick	15	900	0.936	1.72
	Mortar	1.5	1700	1	1.15
Ceiling	Mortar	1	1700	1	1.15
	heavy concrete	15	2300	0.92	1.75
	Mortar	1	1700	1	1.15
Floor	heavy concrete	15	2300	0.92	1.75
	Mortar	2	1700	1	1.15

**Table 2.** Components of the Stone cubicle room

Wall	Composition	e (cm)	$\rho$ (kg/m <sup>3</sup> )	Ci (kJ/ kg.K)	k (W/m.k)
Vertical walls	Gypsum	1.5	1322	1	0.45
	Stone	15	2300	0.94	0.63
	Gypsum	1.5	1322	1	0.45
Ceiling	Gypsum	1	1322	1	0.45
	Stone	15	2300	0.94	0.63
	Gypsum	1	1322	1	0.45
Floor	Gypsum	2	1322	0.94	0.45
	Stone	15	2300	1	0.63

was created to facilitate air movement between the inside and outside of the room through the inclined solar chimney channel. The solar chimney is designed as a rectangular structure, with the face of the chimney oriented southward, measuring 1 m in height and 0.6 m in width. The effect of the air gap was studied with two gap sizes of 0.15 m and 0.25 m, and the solar device was positioned at angles of 30°, 45°, and 60° relative to the horizontal, depending on the specific context under examination. The chimney is constructed from an aluminum frame and a front glass cover, with an absorber located opposite the cover, as depicted in Figure 2(a). The absorber, made from a 1.5 mm thick steel sheet and coated with a dark black color to enhance its ability to absorb incident radiation, was insulated with polystyrene to reduce heat loss and improve the chimney's efficiency.

#### Measured Parameters

In this study, the authors measured various parameters surrounding the experimental setup, including temperature, air velocity, solar intensity, and relative humidity. Indoor temperature, ambient temperature, and internal temperature of the solar chimney were recorded. Air temperature measurements were conducted at the center of the room, as illustrated in Figure 2(b). Temperature measurements were performed at various locations within the chimney and rooms using six T-type K thermocouples. Figure 2(b) provides a detailed illustration of the locations where the thermocouples were placed. Specifically, thermocouples were affixed to the middle of the absorber and glass surface, the

chimney inlet, the window, and one to measure the ambient temperature. The measuring instruments included two Frederiksen 4890.20 solar radiation meters. The first pyranometer was placed on the outer face of the glass cover to measure the received solar intensity, while the second was positioned to measure the solar intensity received by the absorber. Both pyranometers were aligned with the angle of the solar chimney. Air velocities at the inlet and outlet of the solar chimney, inside the room, at the window, and the wind velocity outside were measured using an AVM-10 Hot Wire Anemometer. The UNI-T UT333BT hygrometer was used to measure the relative humidity indoors and outdoors. The output signals from the thermocouples were transmitted to a DATAQ DATA LOGGER data acquisition system, and the results were recorded on a computer. Additionally, a weather station was installed near the experimental setup to simultaneously record weather data such as ambient temperature, solar intensity, and wind speed. The characteristics of the instruments used to measure the parameters are shown in Table 3.

#### Performance Metric

The current investigation employs air change per hour (ACH) as a performance metric, as specified by ANSI/ASH-RAE in 2004. The preceding quantities are provided as follows:

$$Q = v \times A_{\text{solar chimney}} \quad (1)$$

**Table 3.** Equipments/Instruments used for measuring the parameters

Equipments/instruments	Model	Accuracy
Thermocouples	T-type K	±0.3°C
Pyranometer	Frederiksen 4890.20	5%
Anemometer	AVM-10 Hot Wire	±0.05 m/s
Relative humidity meter	UNI-T UT333BT	±5% RH
Data acquisition system	DATAQ DATA LOGGER Model DI-245	± 0.25°C

$Q$  : volumetric flow rate,  $v$ : air velocity and  $A_{solar\ chimney}$ : cross-sectional vector area of solar chimney.

$$ACH = (Q \times 3600)/V_{room} \quad (2)$$

$V_{room}$  indicates the volume of the room where the solar chimney is connected. The air change per hour (ACH) depends on the room size ratio to the chimney area. The value of living room volume ( $V_{room}$ ) in real life is  $27\ m^3$ , calculated using the dimensions of a standard living space measuring  $3\ m \times 3\ m \times 3\ m$ .

In the equation presented, the typical room volume is substituted with a realistic room volume (e.g.,  $27\ m^3$ ) to estimate the ventilation rate in real-life situations. The underlying assumption is that the chamber volume does not affect the volumetric flow rate calculated by the equation. To more accurately represent real-life conditions, volumetric flow rates have been converted to equivalent air changes per hour for a room of  $27\ m^3$ . It is important to note that the air change rate is calculated using Equations (1) and (2).

### System Modelling

The heat balance equations for each component of the solar chimney are the basis for the thermal modeling of the understudied system. Set assumptions have been considered for this:

- The nodal method is considered (the temperature of each layer of the solar device is considered spatially constant).
- Each solid layer's thermo-physical characteristics are assumed to be constant.
- The lateral thermal losses have been ignored.
- The fluid duct pressure losses are neglected.
- The ground-to-solar device radiative heat transfer is disregarded.

The energy conservation concept is applied to each component to forecast the temperatures of each solar device and determine their performances. The following equation commonly expresses this principle.

$$M_i C_i \frac{dT_i}{dt} = \sum_{in} Q_i - \sum_{ou} Q_i \quad (3)$$

where:

- $M_i C_i \frac{dT_i}{dt}$ : the thermal inertia of the component  $i$ .
- $\sum_{in} Q_i$ : total of the energy that component  $i$  received through different heat exchange modes.
- $\sum_{ou} Q_i$  is the total of the energy that component  $i$  lost through different heat exchange modes.

➤ For the glass cover

$$M_g C_g \frac{dT_g}{dt} = A_m [\alpha_g G + h_{r,g-sky}(T_{sky} - T_g) + h_{r,g-p}(T_p - T_g) - h_{v,g-f}(T_g - T_f) + h_{v,a}(T_a - T_g)] \quad (4)$$

The equivalent temperature of the sky is given by the relation [30, 31]:

$$T_{sky} = 0.0552T_a^{1.5} \quad (5)$$

The following correlation can be used to determine the radiative heat transfer coefficient between the glass of a PV module and the sky [32]:

$$h_{r,sky-g} = \sigma \epsilon_g \frac{(T_g^2 - T_{sky}^2)(T_g^2 + T_{sky}^2)}{(T_g - T_a)} \quad (6)$$

The following equation gives the radiative heat transfer coefficient between two parallel flat plates [33, 34]:

$$h_{r,i-j} = \sigma \frac{(T_i + T_j)(T_i^2 + T_j^2)}{\frac{1}{\epsilon_i} + \frac{1}{\epsilon_j} - 1} \quad (7)$$

The convective heat coefficient due to the wind is described by the following relation [35-37]:

$$h_{v,a} = 5.7 + 3.8V_w \quad (8)$$

➤ For the air

$$\dot{m}_f C_f \frac{dT_f}{dx} = 1 [h_{v,f-p}(T_p - T_f) - h_{v,f-g}(T_f - T_g)] \quad (9)$$

The Nusselt number correlation reported by Hollands et al. (1976) is applied in the case of natural convection occurring in an inclined rectangular duct. The following Eq can be used to determine the convective heat transfer coefficient in the air space. This correlation is valid with the following criteria of rectangular duct; tilt angle  $\theta \leq 70^\circ$  and  $H/L \geq 12$  [33, 38, 39, 40]:

$$h_{v,cf} = \frac{k_f}{l_{cf}} Nu = \frac{k_f}{l_{cf}} \left[ 1 + 1.44 \left[ \left( 1 - \frac{1708}{Ra \cos \theta} \right)^+ \left( 1 - 1708 \frac{(\sin 1.8\theta)^{1.6}}{Ra \cos \theta} \right) \right] + \left( \left( \frac{Ra \cos \theta}{5830} \right)^{\frac{1}{3}} - 1 \right)^+ \right] \quad (10)$$

The terms with the sign (+) for this correlation denote that only positive values are considered (i.e. if negative, the 0 is used).

Ra can be expressed as the Rayleigh number, which is:

$$Ra = Gr Pr = \frac{g \beta L^3 \Delta T}{\nu_f^2} Pr = \frac{g \beta L^3 \Delta T}{\nu_f a} \quad (11)$$

where  $g$ ,  $\beta$ ,  $L$ ,  $\nu_f$  and  $a$  are the gravity acceleration, the expansion volume coefficient, the characteristic length ( $l_{cf}$ ), the kinematic viscosity, and the thermal diffusivity  $\left( \frac{k_f}{\rho_f C_f} \right)$ , respectively. All fluid proprieties are calculated using wall mean temperature of the rectangular cavity  $\left( \frac{T_p + T_g}{2} \right)$ .

In the Rayleigh number,  $\Delta T$  is calculated as:

$(T_g - T_f)$  for the exchange fluid-top glass cover, and;  
 $(T_p - T_f)$  for the exchange fluid-bottom glass cover.

The mass flow rate is evaluated by adopting the formula suggested by Bansal et al. (1993) and Arce et al. (2013) [41, 42]:

$$\dot{m}_f = C_d \frac{\rho_f A_o}{\sqrt{1+A_r}} \sqrt{\frac{2gL(T_f - T_r)}{T_r}} \quad (12)$$

Where

$$A_r = \frac{A_o}{2A_{in}} \quad (13)$$

$A_{in}$  and  $A_o$  are the inlet and outlet areas of the chimney.

The experimental investigation of Arce et al. [43] showed that the appropriate value for the discharge coefficient,  $C_d$  is about 0.52:

For the absorber

$$M_p C_p \frac{dT_p}{dt} = A_m [T_g \alpha_p G + h_{r,p-g}(T_g - T_p) + h_{v,p-f}(T_f - T_p) - h_{c,p-in}(T_p - T_{in})] \quad (14)$$

It is easy to express the air temperature along the duct of the chimney as:

$$T_f(x) = \left[ \left( T_{f,in} - \frac{(T_t h_{v,f-t} + T_p h_{v,f-p})}{(h_{v,f-t} + h_{v,f-p})} \right) e^{-\frac{W_c(h_{v,f-t} + h_{v,f-p})x}{\dot{m}_f C_f}} + \frac{(T_t h_{v,f-t} + T_p h_{v,f-p})}{(h_{v,f-t} + h_{v,f-p})} \right] \quad (15)$$

➤ For the absorber plate

$$M_p C_p \frac{dT_p}{dt} = A_c [h_{c,p-in}(T_{in} - T_p) - h_{v,f-p}(T_p - T_f) - h_{r,p-g}(T_p - T_g)] \quad (16)$$

The neighboring solar device parts create a pathway for the conductive heat transfer. The following formula describes how the heat transfer coefficient in this case is stated between two nearby components,  $i$  and  $j$ :

$$h_{c,i-j} = 1 / \left( \frac{l_i}{\lambda_i} + \frac{l_j}{\lambda_j} \right) \quad (17)$$

➤ For the thermal insulator

$$M_{in} C_{in} \frac{dT_{in}}{dt} = A_c [h_{c,in-p}(T_p - T_{in}) - h_{v,a}(T_{in} - T_a)] \quad (18)$$

## RESULTS AND DISCUSSION

Efficient operation of a building's ventilation and air conditioning system ensures human comfort and indoor air quality [44]. In some cases, achieving natural ventilation through external windows can be challenging. As a solution, active ventilation can be employed using alternative methods. This study introduces an active ventilation system that includes an inclined rooftop solar chimney.

Additionally, the windows remain open during the experiment to ensure airflow within the building, as depicted in Figure 2. The system's performance is analyzed for both natural indoor and outdoor airflow.

### Weather Conditions

Figure 3(a) demonstrates the variations in global solar intensity over time during the measurement period. The figure's legend states that the recorded solar intensity values are generally identical across the measurement days. Solar intensity measurements show an increasing trend from 08:00 until reaching a peak around 12:00 noon. Afterwards, the intensity gradually decreases until the end of the measurement period. The highest recorded value of global solar intensity is approximately  $960 \text{ W/m}^2$ , while the largest fluctuation in solar intensity across all measurement days is approximately  $20 \text{ W/m}^2$ . Additionally, the measurements indicate that the wind speed does not exceed  $1.05 \text{ m/s}$  at 3:00 PM, as mentioned in Figure 3(a). Wind speed exhibits diurnal variations, influenced by changes in ambient temperature and solar radiation intensity, gradually increasing from morning to reach its highest point in the afternoon, before decreasing towards the end of the measurement period.

### Impact of Construction Materials

Figure 3(b) illustrates two rooms' outdoor and indoor temperature readings over several days of measurement. The data show that the highest ambient temperature reached  $34^\circ\text{C}$  at 1:00 PM. Moreover, the ambient temperature remained relatively consistent across the different days. Regarding indoor temperature developments, temperature measuring instruments in a hollow brick cavity recorded temperatures ranging from  $19^\circ\text{C}$  to  $34.5^\circ\text{C}$  throughout the day. In contrast, in the other cavity, temperatures fluctuated between  $21^\circ\text{C}$  and  $32.5^\circ\text{C}$ . At 12:00 AM during this experiment, the temperature difference between the two cavities peaked at  $4^\circ\text{C}$ . These measurements suggest that local stone has thermal insulation properties, contributing to energy storage and reducing temperature fluctuations. Throughout the diurnal period, a clear contrast is evident between the temperatures in the two rooms, indicating that the stone helps isolate the interior from the external environment. In contrast, the impact of the external thermal environment is more pronounced within the hollow brick room. The maximum temperature difference between the minimum and maximum temperature in the stone room was  $11.5^\circ\text{C}$ , while in the hollow brick room, it reached up to  $15.5^\circ\text{C}$ . These measurements indicate that the indoor temperature fluctuations in the stone room are due to the thermal inertia of the stone. As the ambient temperature increases, the thermal insulation provided by the stone also increases, leading to a greater temperature difference between the indoor and outdoor environments of the local stone room. Conversely, an increase in ambient temperature for hollow bricks resulted in decreased thermal insulation.

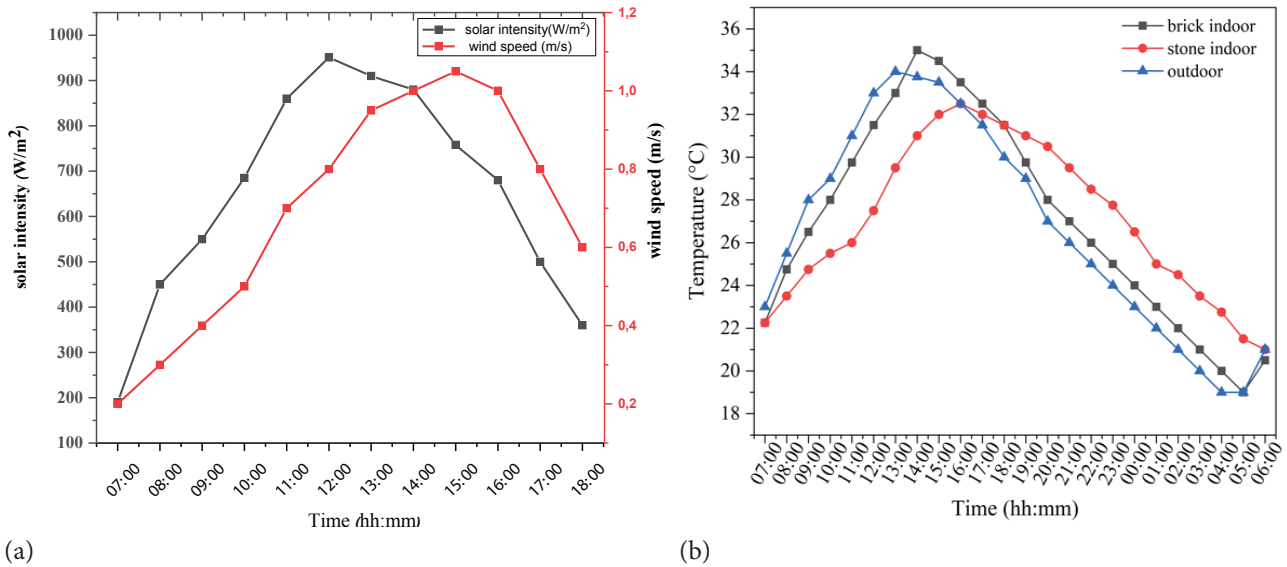


**Figure 3.** Variation of (a) the horizontal solar intensity and wind velocity (b) Variation of the outdoor and indoor temperature of two rooms with time.

**Impact of Solar Radiation on the Chimney**

The efficiency of a solar chimney is influenced by several factors including the amount of solar radiation received by the absorber, the chimney’s inclination angle, and external conditions like wind speed and temperature above the absorber surface. These elements significantly affect the air velocity and the comfort level inside the room. Figure 4(a) captures the variations in solar radiation absorbed during the measurement period, showing an increase from 08:00 AM, peaking around 12:00 noon at approximately 785 W/m², and then declining towards the end. The highest radiation value was observed with a chimney inclined at a 45° angle and featuring a 15 cm air gap. Figure 4(b) shows the variations in

absorber temperature over time for the cases studied. The graph illustrates that the absorber temperature follows the trend of solar intensity evolution, gradually increasing from morning until reaching its peak value of 79.6°C around 12:30 PM. This peak is the highest value recorded in this study for the 45° inclination and a 15 cm air gap. The graph also highlights that the distance between the absorber and the glass pane plays a critical role in solar radiation reception; a smaller air gap of 15 cm results in higher solar intensity and absorber temperatures than a larger gap of 25 cm in all cases studied. As solar intensity decreases, so does the temperature of the absorber, emphasizing the interconnectedness of these variables in influencing chimney performance.

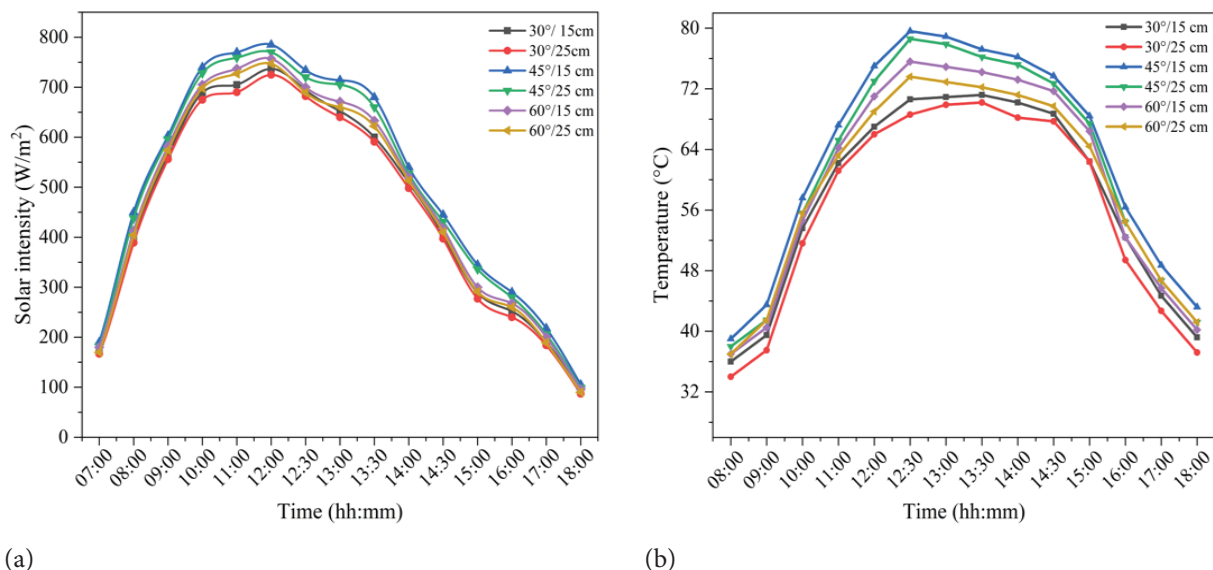


**Figure 4.** Variation of inclined (a) solar intensity and (b) absorber temperatures with time.

**Impact of Solar Chimney on Interior Conditions**

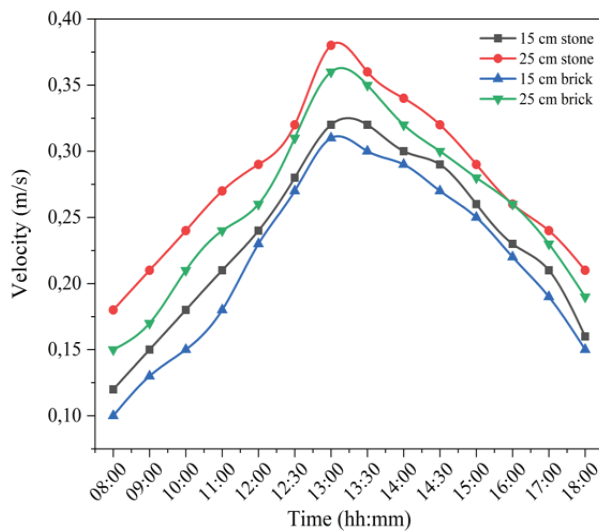
**Impact on ventilated air**

Air exchanges in buildings are crucial role in maintaining human health and thermal comfort, particularly highlighted during the recent COVID-19 pandemic through their impact on indoor environment quality and infection mitigation. Figure 5(a), (b), and (c) depict the variations in inlet air velocity of a solar chimney under different ventilation scenarios in two rooms over the measurement period. The data shows that the average inlet air velocity increases from 08:00 AM until about 01:00 PM, then declines as solar radiation decreases, which reduces the chimney’s performance.

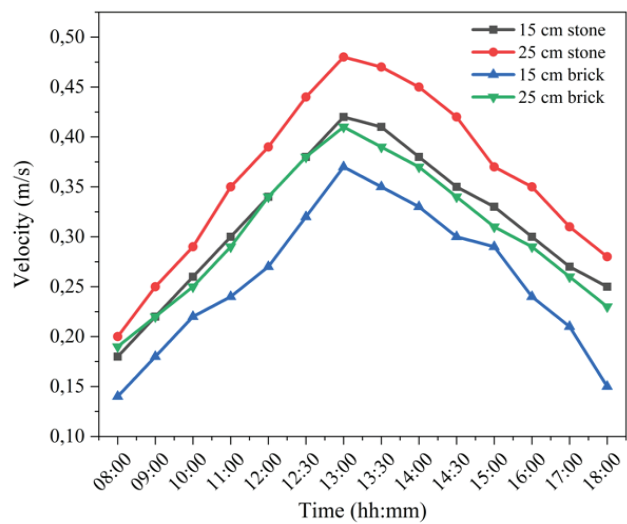
In detail, Figure 5(a) presents the performance of the solar chimney in the local stone room at a 30° inclination with a 25 cm air gap, where the highest inlet velocity reached at 01:00 PM is 0.38 m/s. In comparison, a narrower air gap

of 15 cm at the same inclination achieves a velocity of 0.32 m/s. The velocities for the hollow brick room were 0.36 m/s and 0.31 m/s with a 25 cm and 15 cm gap, respectively, demonstrating that a wider air gap generally enhances chimney performance. Its impact can reach 14 % at peak times. Furthermore, at 45° and 60° inclinations, the 25 cm air gap continues to offer superior performance in both room types compared to the 15 cm gap. Specifically, at a 45° inclination, the velocity can peak at 0.48 m/s in the stone room, and at 60°, it can reach 0.40 m/s. This pattern is consistent across Figure 5(b) and (c), with the 45° inclination achieving higher velocities due to optimal exposure to solar radiation.

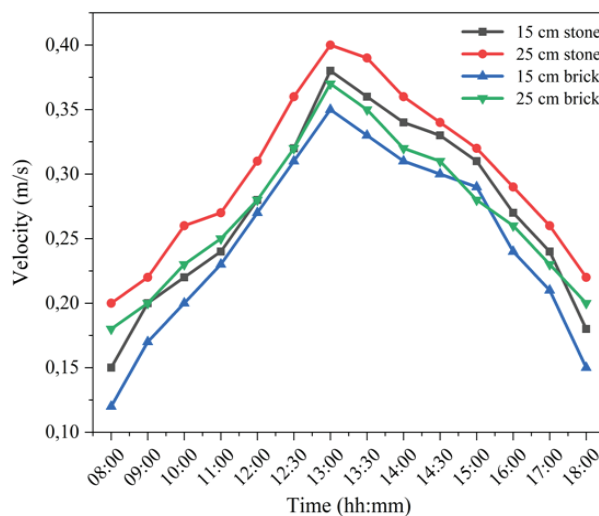
Additionally, the solar chimney performs better in the stone room than in the hollow brick room, where the thermal insulation properties of stone enhance chimney efficiency by about 15%. At an optimal setup of a 45° inclination and a 25 cm air gap, the stone room achieves an inlet



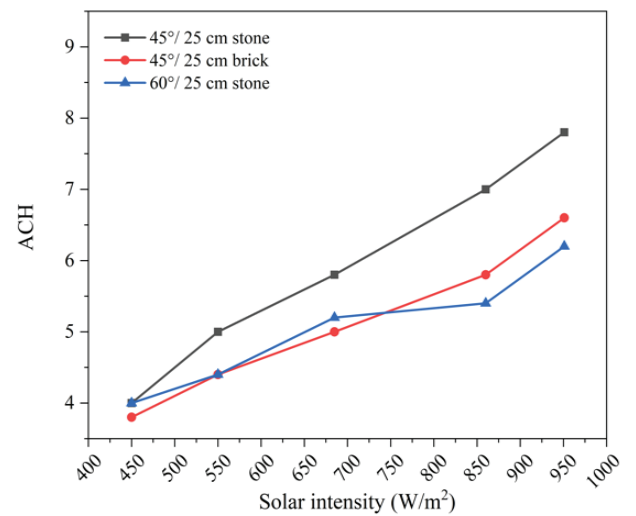
(a) 30°.



(b) 45°.



(c) 60°.



(d)

**Figure 5.** Evolution of Air velocity inlet with time (a,b,c) and (d) ACH and function solar intensity.

air velocity of 0.48 m/s, compared to 0.41 m/s in the hollow brick room. This study underscores the critical role of the chimney’s inclination angle and air gap in optimizing its performance, with a 45° angle and a 25 cm gap outperforming other configurations by up to 20%.

**Impact on ACH**

Figure 5(d) illustrates the relationship between air changes per hour (ACH) and solar energy intensity, where the studied solar chimney is applied in a living room with real dimensions of 3m x 3m x 3m. It highlights the performance of the top three solar chimney cases studied. With increasing solar radiation, the ACH also rises in all scenarios, primarily depending on the strength of the incoming solar radiation. Throughout the day, the ACH induced by the chimney fluctuates between 3 and 7.8, peaking at noon. This high air change rate is attributed to the absorber’s greater absorption of thermal radiation behind the transparent glass, subsequently heating the room air outlet and increasing the buoyancy force.

The experiments demonstrate that a solar chimney with a 25 cm air gap significantly outperforms one with a 15 cm gap in all instances. Solar chimneys with a 45° inclination angle also achieve better ACH than those inclined at 30° or 60°. Specifically, at a 45° inclination and a 25 cm air gap, the ACH reaches its maximum of 7.8 for the stone room with 950 W/m<sup>2</sup> solar radiation intensity. Under similar conditions, the maximum ACH for the brick room is 6.6. In the stone room, with a 60° inclination and the same solar and structural conditions, the ACH reaches 6.2.

Comparatively, the system’s Air Changes per Hour (ACH) with a solar chimney inclined at 45° and with a 25 cm air gap in the stone room is 20% greater than that at a

60° inclination. Furthermore, with a chimney featuring a 25 cm air gap and a 45° inclination, the ACH of the stone room exceeds that of the hollow brick room by 15% [45].

Table 4 presents a comparison between the results obtained in this study, shown in Figure 5(d), and the experimental and numerical findings of Mathur [21], Bassiouny and Koura [46], Abdallah et al. [47] and Haghighi and Maerefat [27]. This study accounted for a wide range of solar intensity variations during the measurement days, considering values of 500,700 and 800 W/m<sup>2</sup>, also used in the aforementioned studies. A summary of these results is presented across various configurations and solar energy densities, highlighting the optimal performance of the solar chimney chosen for each study. The quantitative comparison shows reasonable agreement between the results from this study and those previously published, under various climate conditions.

**Impact on indoor humidity**

Figure 6. shows the indoor relative humidity values in the room during the measurement period for all proposed configurations. The graph illustrates a decrease in relative humidity from 8:00 AM until approximately 1:30 PM, followed by an increase over time. This pattern is because relative humidity tends to decrease with increasing room temperature and rises when the temperature decreases, as concluded from Figure 3(b) and 6. In the room constructed with local stone, the study found that the greatest effect of the chimney on the indoor relative humidity was with an inclination angle of 45° and an air gap of 25 cm. The difference between the lowest and highest relative humidity values across the studied cases was about 6.7%; this effect persisted for most of the day across all cases as shown in

**Table 4.** overview of selected results for comparison with published experimental data

Reference	Research type	Location	Technical specification	Solar intensity (W/m <sup>2</sup> )	ACH (1/h)
Mathur et al. [21]	Experimental	India	Absorber length (m) 0.8 inlet Solar chimney integrated in a room with 1.0 × 0.2 m <sup>2</sup>	500	4.53
				700	5.33
				800	-
Bassiouny and Koura, [46]	Numerical	Minia, Egypt	Absorber length (m) 0.8 inlet Solar chimney integrated in a room with 1.0 × 0.2 m <sup>2</sup> 1.0 × 0.2	500	4.73
				700	5.373
				800	-
Abdallah et al. [47]	Numerical	New Assiut City- egypte	length of the chimney is 2 m with inlet 1.0 × 0.2 m <sup>2</sup> and the inclination angle 50°	500	3.9
				700	4.71
				800	5
Haghighi and Maerefat [27]	Numerical	iran	solar chimney with the length of 3.125 m, width of 4.0 m and air gap of 0.2 m	500	4.72
				700	5.55
				800	-
Present work	Experimental	ouargla-algeria	solar chimney integrated in stone room at 45° and 0.6 × 0.25 m <sup>2</sup>	500	4.56
				700	5.82
				800	6.6

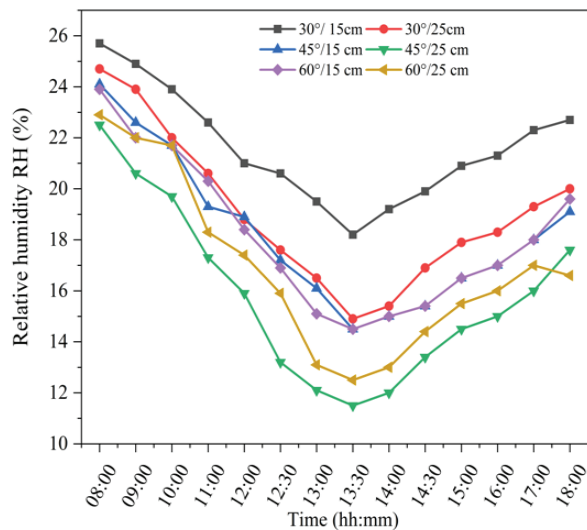
Figure 6(a). In contrast, the difference between the lowest and highest relative humidity values in the hollow brick room was about 3.2%, as shown in Figure 6(b).

The study also found that the maximum indoor relative humidity in the stone room was 27.7% without a solar chimney and 22.4% with a solar chimney. In the hollow brick room, the relative humidity was 23.2% without a chimney and 17.6% with a chimney, as illustrated in Figures 6(c) and (d) (To create an acceptable comfort zone, humidity values should range between 40 and 60%). At 01:30 PM, the lowest humidity recorded using the chimney was 11.5%. As for the room without a chimney, the humidity was 20.5%, a difference of 9% in the local stone room. In the brick room, the difference in humidity between a room equipped with a chimney and without one was 5.4%. As ventilation speed increases, relative

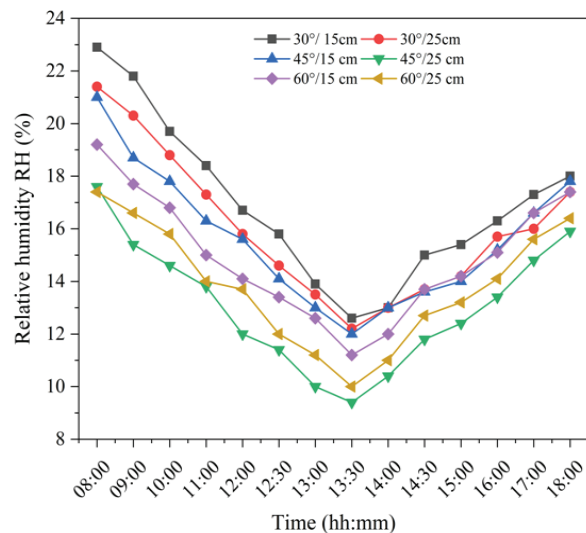
humidity decreases, particularly evident with the solar chimney set at an inclination angle of 45° and an air gap of 25 cm.

**Cost Saving**

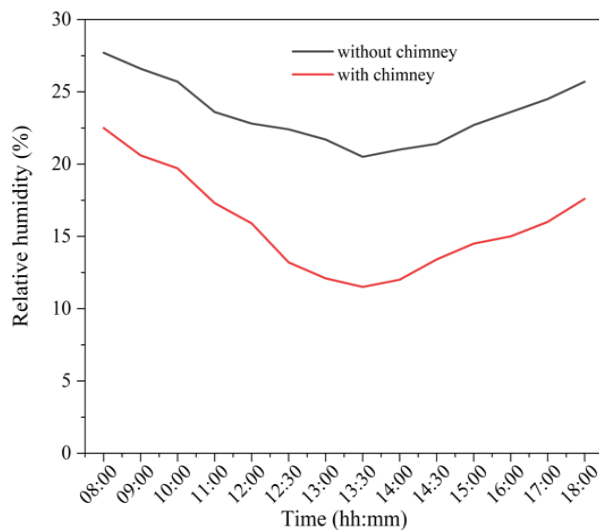
An evaluation of the cost savings from using a solar chimney as a ventilation system was conducted for a living room with an area of 27 m<sup>3</sup>. The analysis involved comparing the energy costs of ventilating this area using mechanical ventilation (fan) versus using energy generated from the solar chimney, based on rates provided by the Algerian Ministry of Electricity (Sonelgaz) [48]. Table 5 illustrates the total energy costs for ventilating a living room during the summer months using mechanical ventilation compared to a solar chimney. An economic study for a family home with three rooms, each equipped with its own ventilation system. The results indicate cost savings ranging



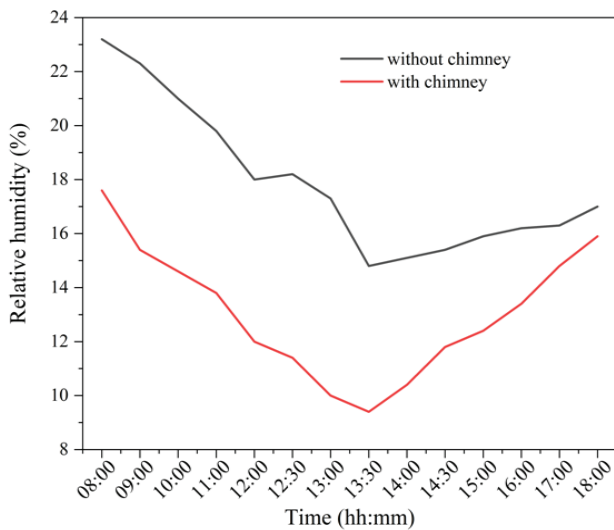
(a)



(b)



(c)



(d)

**Figure 6.** Evolution of rooms’ relative humidity with time (a) local stone (b) hollow brick (c) stone room: with and without chimney (d) brick room: with and without chimney.

**Table 5.** The overall electricity costs used by mechanical ventilation (fan) compared to the solar chimney

Month	ventilation with fan		ventilation with solar chimney				Gain(USD)		
	Living room		Home with 3 rooms		Living room			Home with 3 rooms	
	energy (Kwh)	cost (USD)	cost (USD)	energy (Kwh)	cost (USD)	cost (USD)		cost (USD)	
May	10.8	0.432	1.296	1.68	0.0672	0.2016	1.0944		
June	16.2	0.648	1.944	2.52	0.1008	0.3024	1.6416		
July	19.53	0.7812	2.3436	3.038	0.12152	0.36456	1.97904		
August	18.45	0.738	2.214	2.94	0.1176	0.3528	1.8612		
September	11.25	0.45	1.35	1.75	0.07	0.21	1.14		

from \$1.0944 in May to \$1.97904 in July, with total savings of \$7.71624 over the summer.

### CONCLUSION

This research investigated the thermal behavior of two small rooms constructed from different materials, specifically local stone and hollow brick. Each room featured an integrated rooftop solar chimney designed to optimize ventilation rates. The study measured variables such as indoor air temperature, the velocity of air entering the solar chimney, solar energy intensity, absorbed temperatures, room relative humidity, and overall atmospheric conditions. Various engineering factors that influence system performance were considered, including the solar chimney’s inclination angle, the size of the air gap, and the environmental conditions. The focus was on how these factors affect air changes per hour (ACH), average humidity, and air velocity within the room. Experimental studies on induced natural ventilation were conducted, and the findings were as follows:

1. Optimal Solar Chimney Installation and Design: Solar chimneys with a 45° inclination angle and a 25 cm air gap were shown to be the most effective configuration across various metrics, including air changes per hour (ACH), temperature control, and relative humidity management. This angle aligns optimally with solar radiation patterns to maximize energy absorption, thereby improving the chimney’s ventilation efficiency.
2. Inclination Angle: The angle of inclination is a crucial installation factor that significantly influences the performance of the chimney by affecting the amount of solar radiation the absorber receives. Adjusting this angle can enhance the chimney’s efficiency by up to 20%. Additionally, the air gap, as a configuration factor, contributes to a 14% improvement in performance.
3. Impact of Building Material: The study demonstrated that building materials significantly influence thermal management in buildings, with local stone outperforming hollow bricks in thermal insulation. This results in more stable indoor temperatures and enhances solar chimney efficiency by 15% through improved humidity

control and air exchange rates. The findings highlight the importance of selecting appropriate materials to optimize passive solar ventilation for better energy efficiency and indoor environmental comfort.

4. Solar Radiation as a Driving Force: The effectiveness of the solar chimney is closely tied to the intensity of received solar radiation. Peak ventilation performance corresponds with the highest solar intensities, affirming that solar chimneys are highly effective in regions with abundant sunlight. As solar radiation increases, it boosts the air’s thermal energy within the chimney, enhancing buoyancy and facilitating more effective air exchange.

Finally, the economic analysis offers a promising perspective on cost savings. Utilizing solar chimneys for ventilation significantly lowers energy costs during the summer months, confirming the solar chimney’s role as a sustainable and economically viable option for enhancing indoor environmental quality.

### NOMENCLATURE

$C_i$	Specific heat capacity of a component i (kJ/kg.K)
$D_H$	Hydraulic diameter (m)
$l_i$	Thickness of a component i (m)
$h_c$	Conductive heat transfer coefficient (W/m <sup>2</sup> .K)
$h_r$	radiative heat transfer coefficient (W/m <sup>2</sup> .K)
$h_v$	Convective heat transfer coefficient (W/m <sup>2</sup> .K)
$G$	solar irradiance (W/m <sup>2</sup> )
$Gr$	Grashof number
$L$	Length (m)
$W$	Width (m)
$M_i$	mass of a component i (kg)
$\dot{m}$	mass flow rate (kg/s)
$Pr$	Prandtl number
$Nu$	Nusselt Number
$Ra$	Rayleigh number
$S$	Collector area (m <sup>2</sup> )
$T$	Temperature of a component i (°C)
$t$	Time (s)
$v$	velocity (m/s)
$e$	thickness (cm)

## Greek symbols

$\lambda$	thermal conductivity (W/m.K)
$\tau$	transmissivity
$\alpha$	Absorptivity
$\rho$	Density (kg/m <sup>3</sup> )
$\theta$	tilt angle (Degree (°))
$g$	gravity acceleration
$\beta$	expansion volume coefficient

## Subscripts

<i>ACH</i>	Air changes per hour
<i>a</i>	Ambient
<i>F</i>	Fluid (air)
<i>G</i>	Glass, glazing, gap
<i>Gc</i>	Glass Cover
<i>Gr</i>	Ground
<i>In</i>	Insulator
<i>p</i>	Plate
<i>Th</i>	Thermal
<i>U</i>	Useful
<i>w</i>	Wind
<i>o</i>	outlet

## AUTHORSHIP CONTRIBUTIONS

Authors equally contributed to this work.

## DATA AVAILABILITY STATEMENT

The authors confirm that the data that supports the findings of this study are available within the article. Raw data that support the finding of this study are available from the corresponding author, upon reasonable request.

## CONFLICT OF INTEREST

The authors declared no potential conflicts of interest with respect to the research, authorship, and/or publication of this article.

## ETHICS

There are no ethical issues with the publication of this manuscript.

## REFERENCES

- [1] Algerian Ministry of Energy. National Energy Balance Sheet 2019. 2020 Edition. Algerian Ministry of Energy.
- [2] Ghedamsi R, Settou N, Gouareh A, Khamouli A, Saifi N, Recioui B, et al. Modeling and forecasting energy consumption for residential buildings in Algeria using bottom-up approach. *Energy Build* 2016;121:309-317. [\[CrossRef\]](#)
- [3] Damfeu J.C, Meukam P, Jannot Y, Wati E. Modelling and experimental determination of thermal properties of local wet building materials. *Energy Build* 2017;135:109-118. [\[CrossRef\]](#)
- [4] Ferrante A, Cascella MT. Zero energy balance and zero on-site CO<sub>2</sub> emission housing development in the Mediterranean climate. *Energy Build* 2011;43:2002-2010. [\[CrossRef\]](#)
- [5] Stazia F, Bonfiglia C, Tomassonia E, Di Pernab C, Munafõa P. The effect of high thermal insulation on high thermal mass: is the dynamic behaviour of traditional envelopes in Mediterranean climates still possible. *Energy Build* 2015;88:367-383. [\[CrossRef\]](#)
- [6] Ciampi M, Fantozzi F, Leccese F, Tuoni G. On the optimization of building envelope thermal performance. *Civil Eng Envir Syst* 2003;20:231-254. [\[CrossRef\]](#)
- [7] Jinghua Y, Tian L, Xu X, Wang J. Evaluation on energy and thermal performance for office building envelope in different climate zones of China. *Energy Build* 2015;86W<444:626-39. [\[CrossRef\]](#)
- [8] Khalid BN. External load-bearing walls configuration of residential buildings in Iraq and their thermal performance and dynamic thermal behavior. *Energy Build* 2014;84:169-181. [\[CrossRef\]](#)
- [9] Yüksel A, Arici M, Karabay H. Comparison of thermal response times of historical and modern building wall materials. *J Ther Eng* 2021;7:1506-1518. [\[CrossRef\]](#)
- [10] Shahid M, Karimi MN. Optimization of energy transmittance through building envelope for hot dry climate. *J Ther Eng* 2022;8:595-605. [\[CrossRef\]](#)
- [11] Bekkouche SMA, Benouaz T, Cherier MK, Hamdani M, Benamrane N, Yaiche MR. Thermal resistances of local building materials and their effect upon the interior temperatures case of a building located in Ghardaïa region. *Constr Build Mater* 2014;52:59-70. [\[CrossRef\]](#)
- [12] Cherier MK, Benouaz T, Bekkouche SMA, Hamdani M. Some solar passive concepts in habitat through natural ventilation case study: dry climate in Algeria Ghardaia, *Case Stud Therm Eng* 2018;12:1-7. [\[CrossRef\]](#)
- [13] Hamdani M, Bekkouche SMA, Benouaz T, Cherier MK. A new modelling approach of a multizone building to assess the influence of building orientation in Saharan climate. *Therm Sci* 2015;19:S591-60. [\[CrossRef\]](#)
- [14] Hamdani MZM, Bekkouche SMA, Al-Saadi S, Cherier MK, Djefal R. Judicious method of integrating phase change materials into a building envelope under Saharan climate. *Int J Energy Res* 2021;er.6951. [\[CrossRef\]](#)
- [15] Messaoudi MT, Dokkar B, Khenfer N, Benzid MC. 3D investigation of semi-underground room comfort in a desert climate. *J Ther Eng* 2021;7:1577-1590. [\[CrossRef\]](#)
- [16] Garcia-Hansen V, Esteves A, Pattini A. Passive solar systems for heating, daylighting and ventilation for rooms without an equator-facing facade. *Renew Energy* 2002;26:91-111. [\[CrossRef\]](#)

- [17] Monghasemi N, Vadiie A. A review of solar chimney integrated systems for space heating and cooling application. *Renew Sustain Energy Rev* 2018;81:2714-2730. [\[CrossRef\]](#)
- [18] Zhai XQ, Song ZP, Wang RZ. A review for the applications of solar chimneys in buildings. *Renew Sustain Energy Rev* 2011;15:3757-3767. [\[CrossRef\]](#)
- [19] Khanal R, Lei C. Solar chimney-A passive strategy for natural ventilation. *Energy Build* 2011;43:1811-1819. [\[CrossRef\]](#)
- [20] Afonso C, Oliveira A. Solar chimneys: simulation and experiment. *Energy Build* 2000;32:71-79. [\[CrossRef\]](#)
- [21] Mathur J, Bansal NK, Mathur S, Jain M, Anupma. Experimental investigations on solar chimney for room ventilation. *Sol Energy* 2006;80:927-935. [\[CrossRef\]](#)
- [22] Hamdy I, Fikry M. Passive solar ventilation. *Renew Energy* 1998;14:381-386. [\[CrossRef\]](#)
- [23] Li W, Li Z, Xie L, Li Y, Long T, Huang S, et al. Evaluation of the thermal performance of an inclined solar chimney integrated with a phase change material. *Energy Build* 2022;270:112288. [\[CrossRef\]](#)
- [24] Abdeen A, Serageldin A, Ibrahim MGE, El-Zafarany A, Okawara S, Murata R. Solar chimney optimization for enhancing thermal comfort in Egypt: an experimental and numerical study. *J Sol Energy* 2019;180:524-536. [\[CrossRef\]](#)
- [25] Long S, Guomin Z, Wei Y, Dongmei H, Xudong C, Sujeeva S. Determining the influencing factors on the performance of solar chimney in buildings. *Renew Sustain Energy Rev* 2018;88:223-238. [\[CrossRef\]](#)
- [26] Cao Y, Aldawi F, Sinaga N, Moria H, Dizaji HS, Wae-Hayee M. Single solar chimney technology as a natural free ventilator. energy-environmental case study for Hong Kong. *Case Stud Ther Eng* 2021;26:101173. [\[CrossRef\]](#)
- [27] Haghghi AP, Maerefat M. Solar ventilation and heating of buildings in sunny winter days using solar chimney. *Sust Cit Soc* 2014;10:72-79. [\[CrossRef\]](#)
- [28] Imran AA, Jalil JM, Ahmed ST. Induced flow for ventilation and cooling by a solar chimney. *Renew Energy* 2015;78:236-244. [\[CrossRef\]](#)
- [29] Bisht YS, Pandey SD, Chamoli S. Jet impingement technique for heat transfer enhancement: discovering future research trends. *Energ Source Part A* 2023;45:8183-8202. [\[CrossRef\]](#)
- [30] Al-Nimr MA, Al-Ammari WA. A novel hybrid PV-distillation system. *Sol Energy* 2016;135:874-883. [\[CrossRef\]](#)
- [31] Slimani MEA, Amirat M, Kurucz I, Bahria S, Hamidat A, Chaouch WB. A detailed thermal electrical model of three photovoltaic/thermal (PV/T) hybrid air collectors and photovoltaic (PV) module: comparative study under Algiers climatic conditions. *Energy Conv Manag* 2017;133:458-476. [\[CrossRef\]](#)
- [32] Gholampour M, Ameri M. Energy and exergy analyses of photovoltaic/thermal flat transpired collectors: experimental and theoretical study. *App Energy* 2016;164:837-856. [\[CrossRef\]](#)
- [33] Amori KE, Abd-AlRaheem MA. Field study of various air based photovoltaic/ thermal hybrid solar collectors. *Renew Energy* 2014;63:402-414. [\[CrossRef\]](#)
- [34] Brideau SA, Collins MR. Development and validation of a hybrid PV/thermal air based collector model with impinging jets. *Sol Energy* 2014;102:234-246. [\[CrossRef\]](#)
- [35] Delisle V, Kummert M. A novel approach to compare building-integrated photovoltaics/thermal air collectors to side-by-side PV modules and solar thermal collectors. *Sol Energy* 2014;100:50-65. [\[CrossRef\]](#)
- [36] Joshi AS, Dincer I, Reddy BV. Thermodynamic assessment of photovoltaic systems. *Sol Energy* 2009;83:1139-1149. [\[CrossRef\]](#)
- [37] Slimani MEA., Amirat M, Bahria S, Kurucz I, Aouli M, Sellami R. Study and modeling of energy performance of a hybrid photovoltaic/thermal solar collector: Configuration suitable for an indirect solar dryer. *Energy Convers Manag* 2016;125:209-221. [\[CrossRef\]](#)
- [38] Hollands KGT, Unny TE, Raithby GR, Konicek L. Free convective heat transfer across inclined air layers. *ASME J Heat Transf* 1976;98:189-193. [\[CrossRef\]](#)
- [39] Guo C, Ji J, Sun W, Ma J, He W, Wang Y. Numerical simulation and experimental validation of tri-functional photovoltaic/thermal solar collector. *Energy* 2015;87:470-480. [\[CrossRef\]](#)
- [40] Bahrehmand D, Ameri M. Energy and exergy analysis of different solar air collector systems with natural convection. *Renew Energy* 2015;74:357-368. [\[CrossRef\]](#)
- [41] Bansal N, Mathur R, Bhandari M. Solar chimney for enhanced stack ventilation. *Build Envir* 1993;28:373-377. [\[CrossRef\]](#)
- [42] Arce J, Xamán JP, Alvarez G, Jiménez MJ, Enríquez R, Heras MR. A simulation of the thermal performance of a small solar chimney already installed in a building. *J Sol Energy Eng* 2013;135:1741-1747. [\[CrossRef\]](#)
- [43] Arce J, Jiménez JM, Guzmán JD, Heras MR, Alvarez G, Xamán J. Experimental study for natural ventilation on a solar chimney. *Renew Energy* 2009;34:2928-2934. [\[CrossRef\]](#)
- [44] Rattanongphisat W, Prachaona T, Harfield A, Sato K, Hanaoka O. Indoor climate data analysis based a monitoring platform for thermal comfort evaluation and energy conservation. *Energy Proc* 2017;138:211-216. [\[CrossRef\]](#)
- [45] Hebbal B, Marif Y, Hamdani M, Belhadj MM, Bouguettaia H, Bechki D. The geothermal potential of underground buildings in hot climates: case of Southern Algeria 2021. *Case Study Ther Eng* 2021;28:101422. [\[CrossRef\]](#)

- [46] Bassiouny R, Koura NSA. An analytical and numerical study of solar chimney use for room natural ventilation. *Energy Buildings* 2008;40:865-873. [\[CrossRef\]](#)
- [47] Abdallah ASH, Yoshino H, Goto T, Enteria N, Radwan MM, Eid MA. Integration of evaporative cooling technique with solar chimney to improve indoor thermal environment in the New Assiut City, Egypt. *Inter J Energy Env Eng* 2013;4:45. [\[CrossRef\]](#)
- [48] Sonelgaz, 2021. Available at: <http://www.sonelgaz.dz>. Accessed July 21, 2021.